SMC-TR-02-17

AEROSPACE REPORT NO.
TR-2002(8570)-5

New Cirrus Models for MODTRAN4

I: Models Derived from the Standard and Subvisual Models

28 February 2002

Prepared by

S. MAZUK and D. K. LYNCH
Space Science Applications Laboratory
Laboratory Operations

Prepared for

SPACE AND MISSILE SYSTEMS CENTER
AIR FORCE SPACE COMMAND
2430 E. El Segundo Boulevard
Los Angeles Air Force Base, CA 90245

Engineering and Technology Group

THE AEROSPACE CORPORATION
El Segundo, California

APPROVED FOR PUBLIC RELEASE;
DISTRIBUTION UNLIMITED

This report was submitted by The Aerospace Corporation, El Segundo, CA 90245-4691, under Contract No. F04701-00-C-0009 with the Space and Missile Systems Center, 2430 E. El Segundo Blvd., Los Angeles Air Force Base, CA 90245. It was reviewed and approved for The Aerospace Corporation by J. A. Hackwell, Principal Director, Space Science Applications Laboratory. Michael Zambrana was the project officer for the Mission-Oriented Investigation and Experimentation (MOIE) program.

This report has been reviewed by the Public Affairs Office (PAS) and is releasable to the National Technical Information Service (NTIS). At NTIS, it will be available to the general public, including foreign nationals.

This technical report has been reviewed and is approved for publication. Publication of this report does not constitute Air Force approval of the report's findings or conclusions. It is published only for the exchange and stimulation of ideas.

Michael S. Zambrana

Michael Zambrana
SMC/AXE

REPORT DOCUMENTATION PAGE

Form Approved
OMB No. 0704-0188

1. REPORT DATE (*DD-MM-YYYY*)
28-02-2002

2. REPORT TYPE

3. DATES COVERED (*From - To*)

4. TITLE AND SUBTITLE

New Cirrus Models for MODTRAN4

I: Models Derived from the Standard and Subvisual Models

5a. CONTRACT NUMBER
F04701-00-C-0009

5b. GRANT NUMBER

5c. PROGRAM ELEMENT NUMBER

5d. PROJECT NUMBER

5e. TASK NUMBER

5f. WORK UNIT NUMBER

6. AUTHOR(S)

Steve Mazuk and David K. Lynch

7. PERFORMING ORGANIZATION NAME(S) AND ADDRESS(ES)

The Aerospace Corporation
Laboratory Operations
El Segundo, CA 90245-4691

8. PERFORMING ORGANIZATION REPORT NUMBER

TR-2002(8570)-5

9. SPONSORING / MONITORING AGENCY NAME(S) AND ADDRESS(ES)
Space and Missile Systems Center
Air Force Space Command
2450 E. El Segundo Blvd.
Los Angeles Air Force Base, CA 90245

10. SPONSOR/MONITOR'S ACRONYM(S)
SMC

11. SPONSOR/MONITOR'S REPORT NUMBER(S)
SMC-TR-02-17

12. DISTRIBUTION/AVAILABILITY STATEMENT

Approved for public release; distribution unlimited.

13. SUPPLEMENTARY NOTES

14. ABSTRACT

The purpose of this report is to set forth a new set of cirrus cloud models for use with the MODTRAN4 atmospheric transmission model and to provide a wider range of cirrus models with which to investigate future remote sensing techniques that may have to observe through cirrus. The cirrus cloud models were derived by selecting mode particle sizes between and beyond the two existing cirrus cloud models in MODTRAN4: Standard (mode particle radius 64 μm) and subvisual (mode 4 μm). The new set of models consists of 70 models whose mode particle radius range between 0.1 and 64 μm. The format of the models meets the input requirements for MODTRAN4 and consist of files containing the input information on card 2E2. All the model calculations are based on spherical particles.

15. SUBJECT TERMS
Cirrus, Scattering, Absorption, Extinction, Clouds

16. SECURITY CLASSIFICATION OF:			17. LIMITATION OF ABSTRACT	18. NUMBER OF PAGES	19a. NAME OF RESPONSIBLE PERSON
a. REPORT	b. ABSTRACT	c. THIS PAGE			Steve Mazuk
UNCLASSIFIED	UNCLASSIFIED	UNCLASSIFIED		21	19b. TELEPHONE NUMBER *(include area code)* (310)336-5614

Contents

Figures

Table

1. Introduction

The purpose of this report is to set forth a new set of cirrus cloud models for use with the MODTRAN4 atmospheric transmission model and to provide a wider range of cirrus models with which to investigate future remote sensing techniques that may have to observe through cirrus. The cirrus cloud models were derived by selecting mode particle sizes between and beyond the two existing cirrus cloud models in MODTRAN4: Standard (mode particle radius 64 μm) and subvisual (mode 4 μm.) The new set of models consists of 70 models whose mode particle radius range from between 0.1 and 64 μm. The format of the models meets the input requirements for MODTRAN4 and consist of files containing the input information on card 2E2. All the model calculations are based on spherical particles. A plan is included for extending the models to more realistic ones that use nonspherical particles.

The Moderate Resolution Transmittance (MODTRAN) code developed by the Air Force Research Lab (AFRL) calculates atmospheric transmittance and radiance for frequencies from 0 to 50,000 cm^{-1} at moderate spectral resolution, primarily 2 cm^{-1} (20 cm^{-1} in the UV) (Berk et al. 1989). The development of the MODTRAN model was motivated by the need for higher spectral resolution than was available in the Low Resolution Transmittance (LOWTRAN7) (Kneizys et al. 1986). MODTRAN's capabilities include spherical refractive geometry, solar and lunar source functions, scattering (Rayleigh, Mie, single and multiple), and default atmosphere profiles (gases, aerosols, clouds, fogs, and rain). MODTRAN, version 4, release 1 was used for these calculations, and is the most current release.

The Cirrus cloud models in MODTRAN, and its predecessor LOWTRAN, were calculated by Shettle et al. (1988) using the optical constants for water ice measured by Warren (1984). These are known as the "Standard" and "Subvisual" Cirrus cloud models. The shape of the ice crystals was approximated using spherical particles, allowing the use of Mie theory to calculate the absorption and extinction (Bohren 1983, van de Hulst 1957). Shettle et al. assumed a particle size distribution given by the log-normal distribution function:

$$dN/d\mathcal{a} = n(\mathcal{a}) = a\mathcal{a}\exp(-b\mathcal{a}), \qquad (1)$$

where $\mathcal{a}$ is the particle radius, and a and b are constants. Figure 1 shows the particle size distributions used to compute K_E for the standard and subvisual models. The mean (mode) particle radius for the standard and subvisual models is 64 μm and 4 μm, respectively, and the calculations were done under the assumption that all the particles are spherical. The particles were treated individually between 0.05 μm and 1000 μm with 799 interspaced sizes.

The term "cirrus" is used to describe a number of clouds with similar characteristics (Lynch and Sassen 2001), the main difference within the cirrus category being particle size. In a previous study,

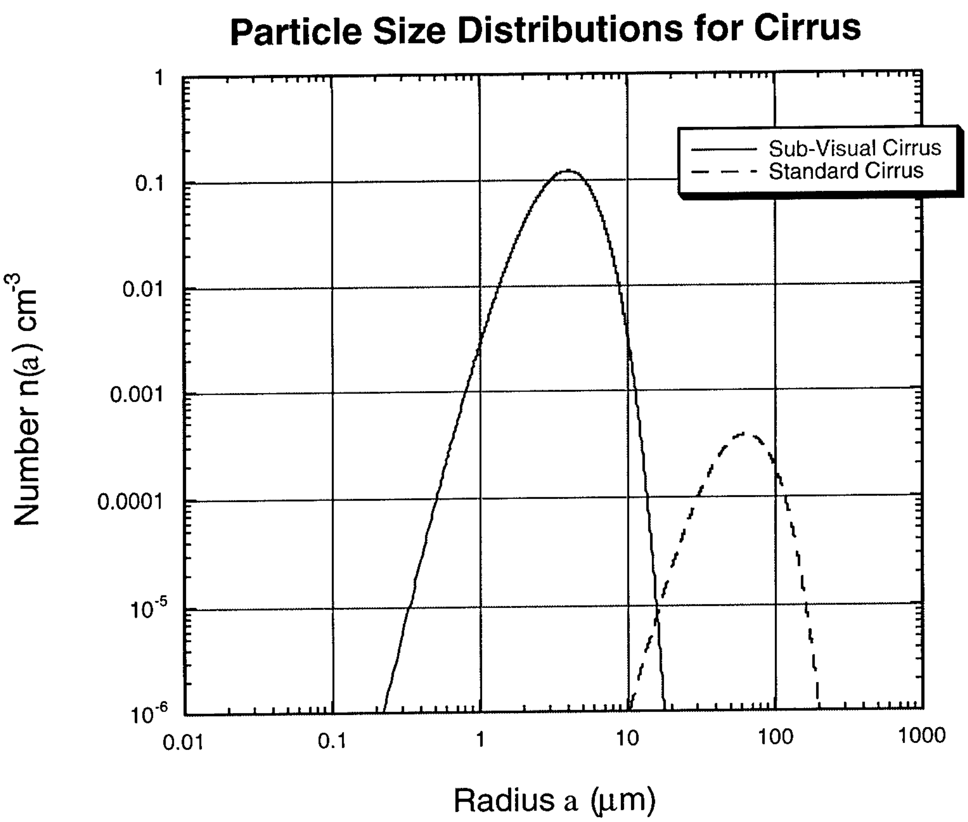

Figure 1. The particle size distribution for the subvisual model contains more particles cm^{-3}, and they are on average much smaller ($a_{mode} = 4$ μm) than for the standard model ($a_{mode} = 64$ μm).

Lynch and Mazuk (2000) discussed how the particle size distribution has a strong influence on the absorption and emission spectra for a particle cloud. The paper by Fu (1996) summarizes 25 distinct particle size distributions that have been experimentally measured in cirrus clouds. Fu also notes that the particle size distributions are difficult to measure experimentally. Small ice particles are particularly difficult to measure, and in some experiments, the distribution functions were extrapolated to small sizes from measurements of larger particles.

2. Derivation of the New Models

The new cirrus models fill in the mode particle sizes between the two existing cirrus models and extend the subvisual cirrus model to smaller particle sizes than have previously been available. The same modeling methods used by Shettle et al. (1988) were used here. The Mie scattering code of Shettle et al. was used along with the optical constants of Warren (1984) to generate a set of extinction coefficient (K_E, km^{-1}), absorption coefficient (K_A, km^{-1}), and asymmetry parameter (g), all as a function of wavelength between 0.4 and 14.7 μm.

3. The New Models

The new cirrus cloud models consist of a large amount of numerical tabulations of extinction, absorption, and asymmetry coefficients. Therefore, we show them here in graphical form in Figures 2–15. The actual numerical models will be in the form of MODTRAN card 2E2 (See below) and will be transferred electronically. In each of Figures 2–9, the standard cirrus model corresponds to the far edge of the plot (a_{MODE} = 64 μm), and the subvisual cirrus model corresponds to the near edge (a_M = 4 μm). In each of Figures 10–17, the subvisual cirrus model corresponds to the far edge of the plot (a_M = 4 μm).

Figure 2 shows a surface plot of the extinction coefficient K_E over the wavelength range of 0.4 to 14.7 μm. This is normalized to unity at 0.55 μm for all mode particle sizes, but can be rescaled according to the user's selection of optical depth. Note that K_E is relatively flat and unstructured except in the foreground where the small particle effects become evident. The two obvious valleys correspond to the vibrational structure of ice at 3.16 μm and the broader rotational structure around 10.5 μm.

Figure 3 shows a surface plot of the absorption coefficient K_A over the wavelength range of 0.5 to 14 μm. Here, there is considerably more structure in both wavelength and mode particle size space, and as in Figure 2, the structure increases with decreasing particle size.

Figure 2 is relatively flat because the extinction is dominated by scattering, and scattering efficiency is not strongly dependent on particle size or wavelength. In fact, it depends on the scattering size parameter $X = 2\pi a/\lambda$, which is generally greater than unity for most of the situations shown in the figure. The ample structure in Figure 3, on the other hand, is the result of numerous variations in the optical constants of ice. These are embodied in the absorption size parameter $\Omega = 4\pi k a/\lambda$ (Lynch and Mazuk 1998), where k is the imaginary part of the index of refraction. In this situation, $\Omega << 1$, and, therefore, the variations in k become dominant.

The asymmetry parameter g results are shown in Figure 4, showing similar structure. There is considerable structure, but unlike the values in Figure 3, g's dynamic range is fairly small, generally falling in the range of 0.8 to 1.0. As a_M decreases, the particles become small compared to the wavelength, and the X drops below unity. When this happens, the particles become more like "Rayleigh" particles, and g approaches zero.

Figures 5, 6, and 7 are expanded version of Figure 2, 3, and 4. These figures show the extinction, absorption, and asymmetry parameters between 1 and 1.5 μm. In Figure 5, the extinction, K_E, is relatively flat, although some size- and wavelength-dependent "warpage" is present. Figure 6 shows virtually no variation in the absorption K_A, but Figure 7 shows significant variation in g as a function of mode radius a_M.

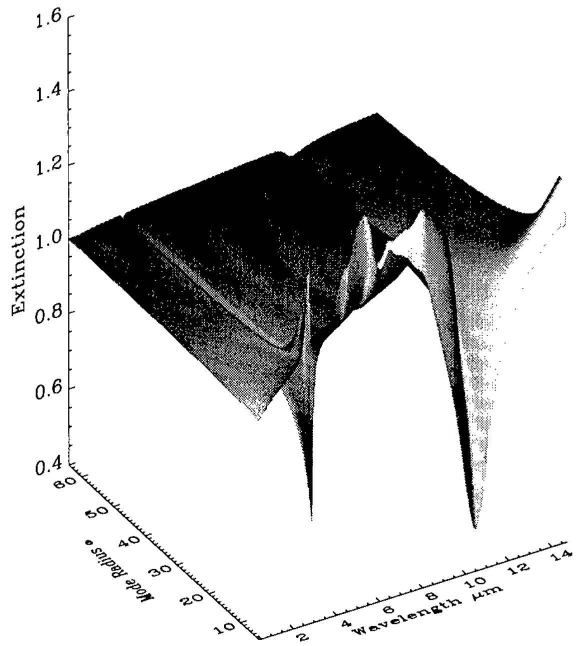

Figure 2. Extinction coefficient (K_E km^{-1}): $\lambda = 0.5$ to 14 µm, and $a_M = 4$ to 64 µm.

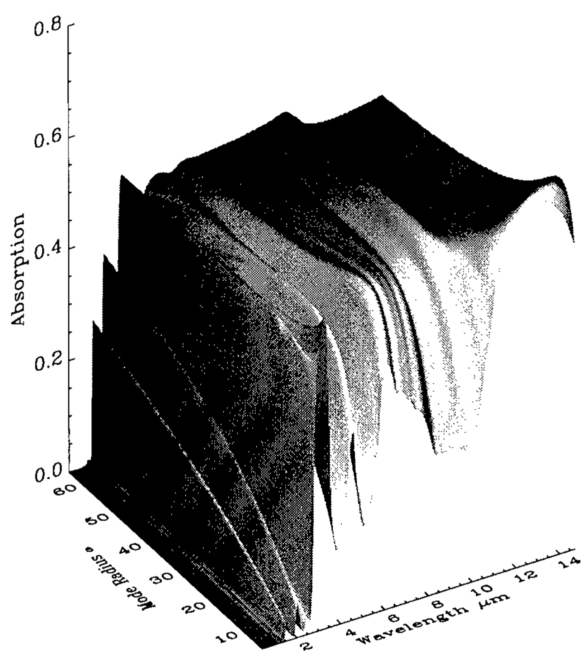

Figure 3. Absorption coefficient (K_A km^{-1}): $\lambda = 0.5$ to 14 µm, and $a_M = 4$ to 64 µm.

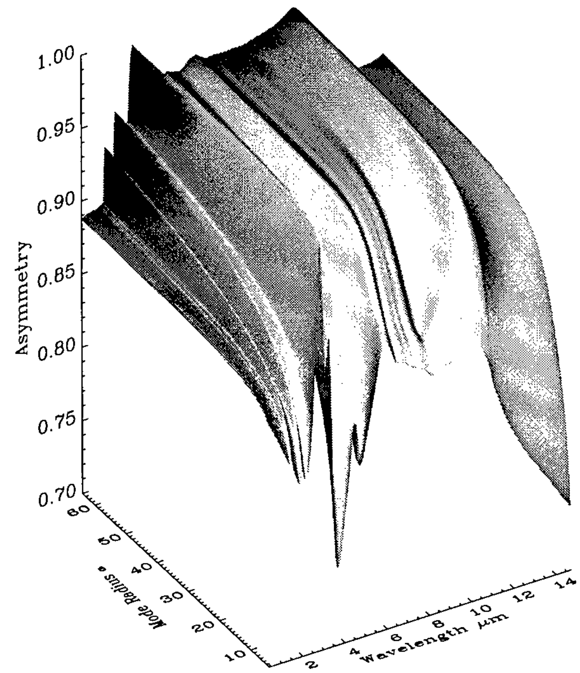

Figure 4. Asymmetry parameter (g, unitless): $\lambda = 0.5$ to 14 μm, and $a_M = 4$ to 64 μm.

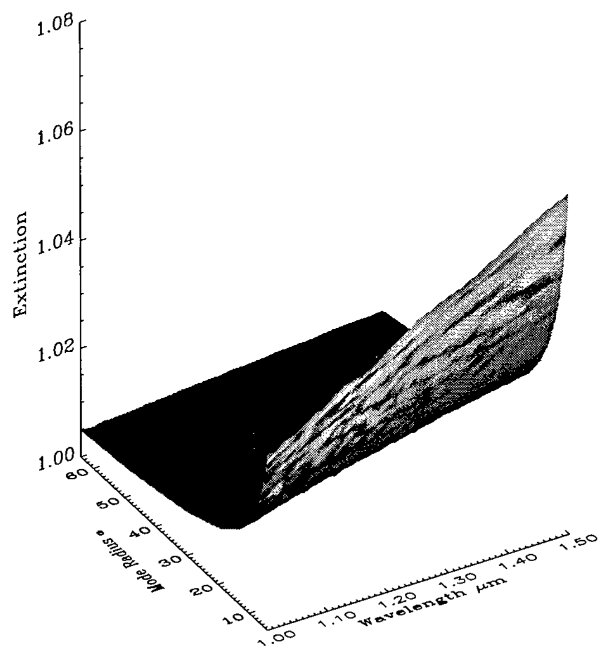

Figure 5. Extinction coefficient (K_E km^{-1}): $\lambda = 1.0$ to 1.5 μm, and $a_M = 4$ to 64 μm.

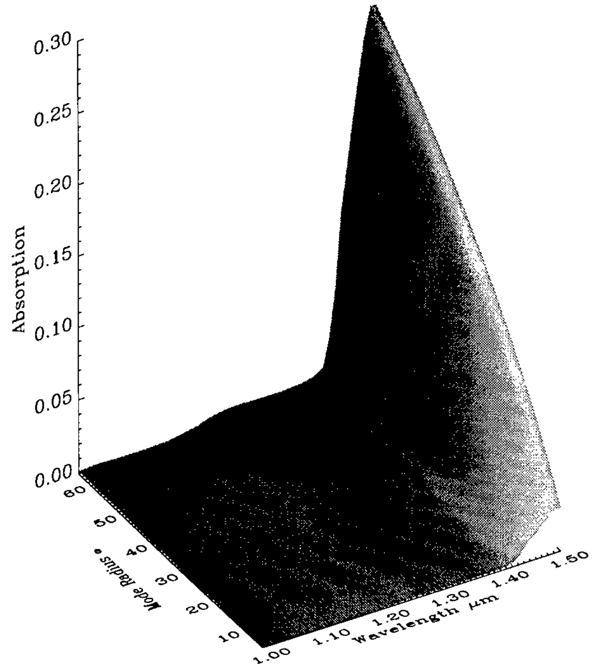

Figure 6. Absorption coefficient (K_A km^{-1}): $\lambda = 1.0$ to 1.5 μm, and $a_M = 4$ to 64 μm.

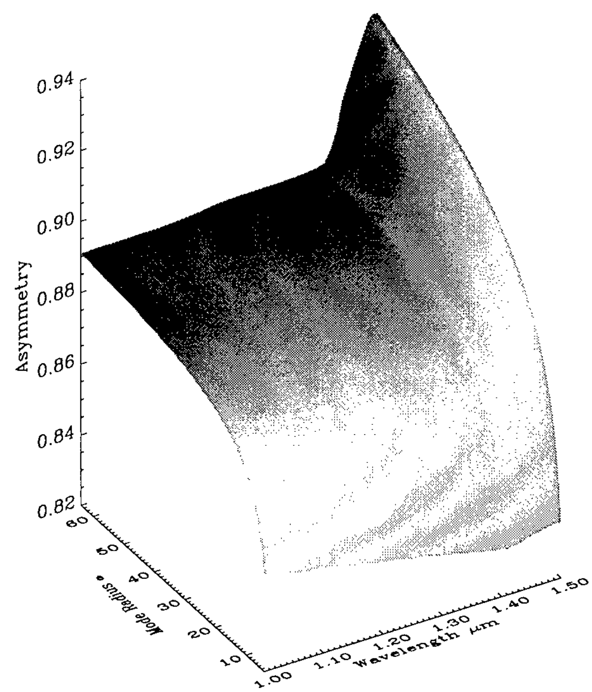

Figure 7. Asymmetry parameter (g, unitless): $\lambda = 1.0$ to 1.5 μm, and $a_M = 4$ to 64 μm.

Figures 8 and 9 show the scattering coefficient K_S, which is defined as $K_E - K_A$. They are included for completeness.

It is clear from all of the above results that changes in the mean particle size (i.e., changes in a_M) have the greatest influence for small particles. This sensitivity is well known and has been discussed in the context of cirrus clouds by Takano et al. (1992). Therefore, we extended the range of values for a_M downward to between 0.1 and 4.0 μm and calculated K_E, K_A and g. The results are shown in Figures 10–17, and correspond to Figures 2–9, except they are for smaller particles. In each of Figures 10–17, the subvisual cirrus model corresponds to the far edge of the plot ($a_M = 4$ μm).

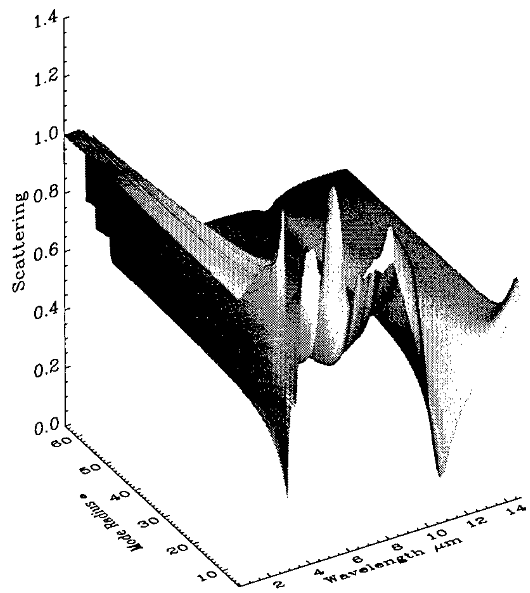

Figure 8. Scattering coefficient (K_E km^{-1}): $\lambda = 0.5$ to 14 μm, and $a_M = 4$ to 64 μm.

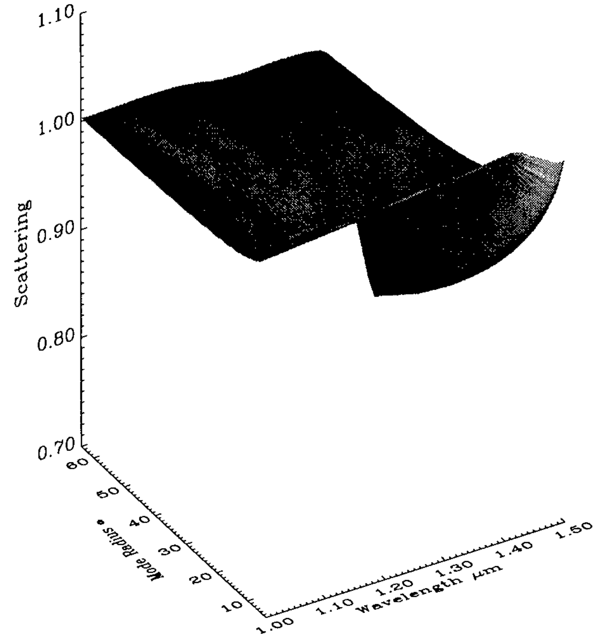

Figure 9. Scattering coefficient (K_E km^{-1}): $\lambda = 1.0$ to 1.5 μm, and $a_M = 4$ to 64 μm.

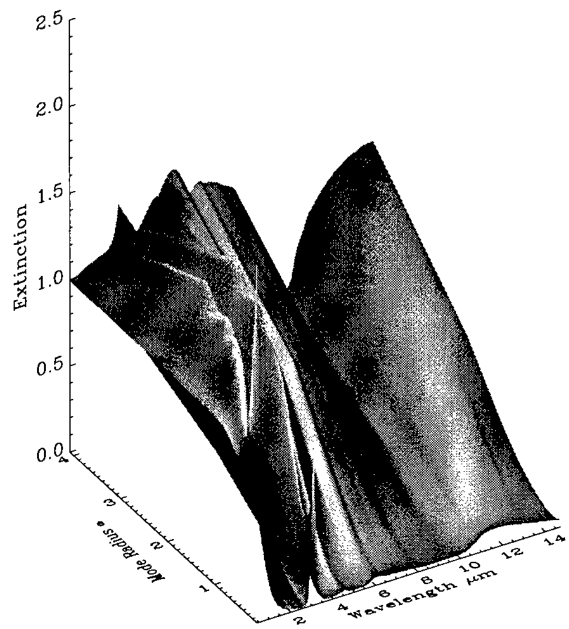

Figure 10. Extinction coefficient (K_E km^{-1}): $\lambda = 0.5$ to 14 μm, and $a_M = 0.1$ to 4 μm.

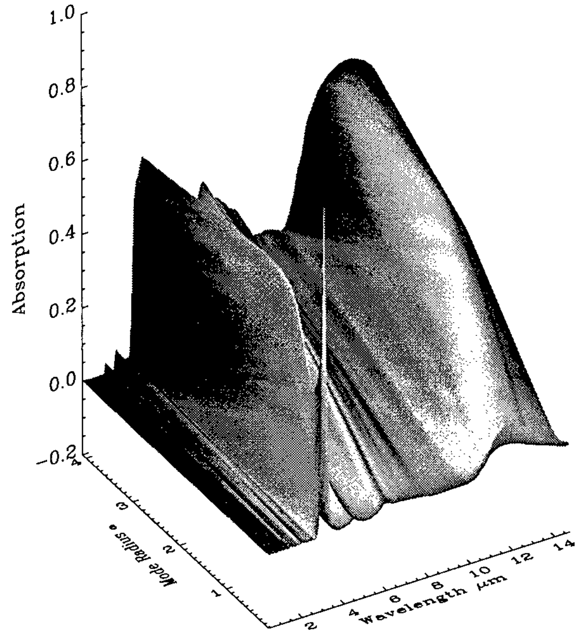

Figure 11. Absorption coefficient (K_A km^{-1}): λ = 0.5 to 14 μm, and a_M = 0.1 to 4 μm.

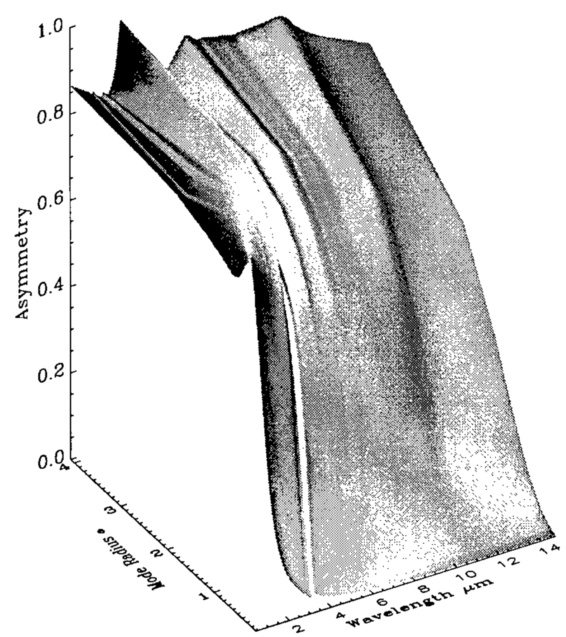

Figure 12. Asymmetry parameter (g, unitless): λ = 0.5 to 14 μm, and a_M = 0.1 to 4 μm.

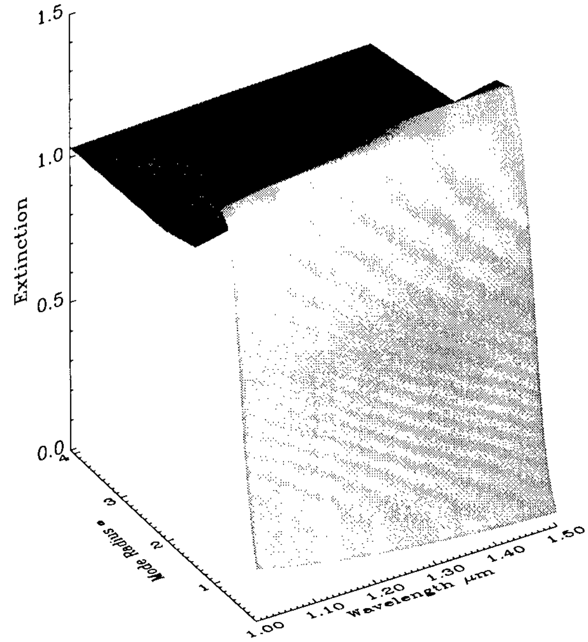

Figure 13. Extinction coefficient (K_E km^{-1}): $\lambda = 1.0$ to 1.5 μm, and $a_M = 0.1$ to 4 μm.

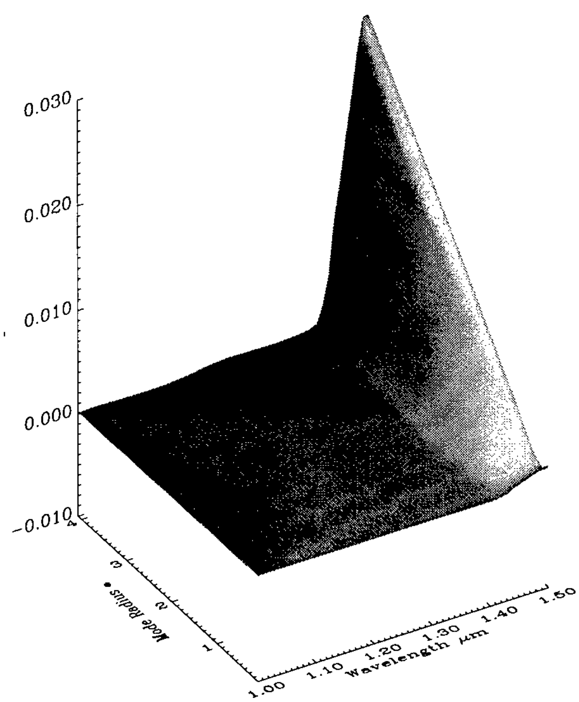

Figure 14. Absorption coefficient (K_A km^{-1}): $\lambda = 1.0$ to 1.5 μm, and $a_M = 0.1$ to 4 μm.

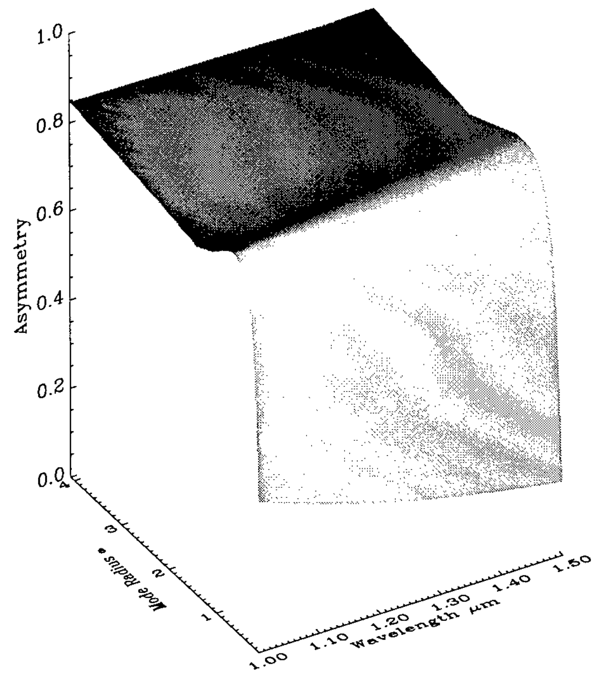

Figure 15. Asymmetry parameter (g, unitless): $\lambda = 1.0$ to 1.5 μm, and $a_M = 0.1$ to 4 μm.

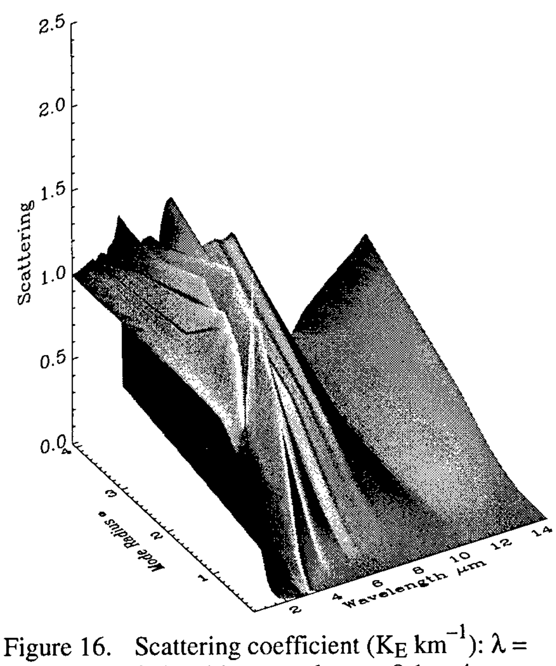

Figure 16. Scattering coefficient (K_E km^{-1}): $\lambda =$ 0.5 to 14 μm, and $a_M = 0.1$ to 4 μm.

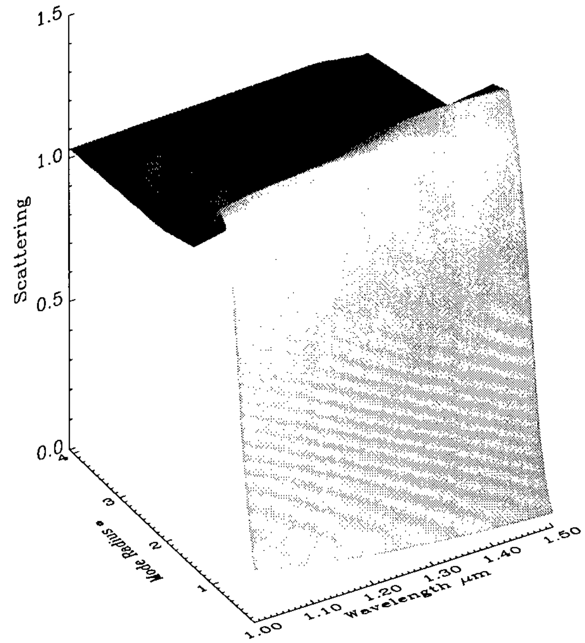

Figure 17. Scattering coefficient (K_E km^{-1}): $\lambda = 1.0$ to 1.5 μm, and $a_M = 0.1$ to 4 μm.

4. Using the New Models in MODTRAN4

The new cirrus cloud models were developed for use with the MODTRAN4 atmospheric transmission model. MODTRAN4 allows for the insertion of a cloud model, which is then used in conjunction with model (or measured) atmospheric data in the calculation of transmission and radiance. Inputs to MODTRAN4 consist of lines of formatted ASCII text, and are referred to as "cards" in reference to IBM punch cards formerly used as computer inputs.

The cloud and aerosol specification begins on Card 2. Here, we commonly set the parameter IHAZE = 1 for a rural aerosol model with 23 km visibility. We also set ICLD = 1 to select a cumulus cloud. Remaining values are set to zero, but the user can make further selections depending on the characteristics of a particular analysis.

Card 2A (alternate form used if ICLD = 1 through 10) defines the parameters for the cloud model chosen on Card 2, and is used for clouds other than cirrus. Entries on this card trigger the reading of cards 2E1 and 2E2. The simplest way to define a cirrus cloud is to specify its base height and thickness (both in km) and its extinction coefficient, K_E, from the calculated models. In this mode, however, the thickness must be chosen so as to give the proper optical depth at 0.55 μm. The optical depth, τ, and K_E are simply related through the cloud thickness,

$$\tau = K_E L,$$

where L is the cloud thickness in km. The user also sets the number of layer boundaries used to define the cloud structure on card 2E1, and the number of wavelengths to be input for cloud extinction and absorption values on card 2E2. The cloud column water density is set to zero. Finally, the user specifies the model asymmetry values rather than defaulting to Henyey-Greenstein values.

Card 2E1 defines the cloud layer's ice and liquid water densities in g/m^3. As it happens, the value of densities are not used directly; so as long as they are greater than zero, the code will work. *For cirrus clouds only, the user must zero out the water density* and the rain rate as well.

Card 2E2 defines the extinction, absorption, and asymmetry of water and ice for each wavelength (Table 1). Here, the user must input negative values for the water, which causes the cloud model to use the default extinction, absorption, and asymmetry values for the cloud we specified in Card 2 (here a cumulus cloud). But recall that the user previously zeroed out the water content of the cloud, so there is no contribution here. So the only values that should be active are the ones input for the ice based on the models presented here.

Table 1. Sample input Card 2E2

		Units	
1.38	Wavelength	(μm)	
−9	Extinction coefficient	(km^{-1})	for water (negative suppresses water cloud)
−9	Absorption coefficient	(km^{-1})	for water (negative suppresses water cloud)
−9	Asymmetry parameter	(unitless)	(negative suppresses water cloud)
0.1	Extinction coefficient	(km^{-1})	for ice (typical)
0.01	Absorption coefficient	(km^{-1})	for ice (typical)
0.86	Asymmetry parameter	(unitless)	for ice (typical)

5. Limitations of the Models

The models presented here are based on Shettle et al.'s cirrus cloud models. They give reasonable results and reproduce the basic properties of cirrus clouds, i.e., absorption peaks at the appropriate places, representative transmission, scattering cross sections that behave as expected, etc. To the extent to which the two models in MODTRAN4 are useful, the models presented here extend this utility to intermediate size regimes and, perhaps more importantly, to smaller sizes that are associated with subvisual cirrus. For most applications, they are about as good as can be achieved within the computational limitations of MODTRAN.

All the new cirrus cloud models, as well as the built-in cirrus cloud models, suffer from one major limitation: they are calculated assuming that the clouds are composed of spherical particles. The ice particles comprising cirrus clouds are unquestionably non-spherical, often highly so. The impact of the spherical particle assumption is that the scattering of light is not accurately calculated over all angles; i.e., the bi-directional reflectance distribution function (BRDF) is not well modeled. However, the current release of the MODTRAN4 model does not allow insertion of a BRDF for any cloud model; only ground surface BRDFs can be inserted, so this solution is not available. The alternative is to parameterize the effects of non-spherical particles within the limitations of the MODTRAN inputs. This approach will be explored in the next phase of our modeling efforts.

6. Conclusions

We have produced a new set of cirrus cloud models for use with the MODTRAN atmospheric transmission code. These models extend the range of mean particle sizes beyond the limits of the existing models included in MODTRAN, covering the broader range of cloud composition seen in nature. These models can be used in conjunction with MODTRAN to investigate the effects of cirrus clouds on future remote sensing techniques that may have to observe through cirrus.

References

Berk, L. S. Bernstein, and D. C. Robertson, MODTRAN: A Moderate Resolution Model for LOWTRAN 7 (1989), Air Force Geophysics Laboratory Technical Report GL-TR-89-0122, Hanscom AFB, MA.

Bohren, C. F. and D. R. Huffman, *Absorption and Scattering of Light by Small Particles*, 1983, Wiley, New York.

Fu, Quang, "An accurate parameterization for the solar radiative properties of cirrus clouds for climate models," *Journal of Climate*, **9**, pp. 2058–2082, 1996.

Kneizys, F. X., Shettle, E. P., Abreu, L. W., Chetwynd, J. H., Anderson, G. P., Gallery, W. O., Selby, J. E. A., and Clough, S. A., *Users Guide to LOWTRAN 7*, Tech. rep., Air Force Geophysics Laboratory AFGL 1986.

Lynch, D. K. and Sassen, K., "Subvisual Cirrus," *CIRRUS*, D. K. Lynch, K. Sassen, D. Starr, and G. Stephens, eds, Oxford University Press, 2001

Lynch, D. K., K. Sassen, D. Starr, and G. Stephens (editors), *CIRRUS*, Oxford University Press, Oxford (2001).

Lynch, D. K. and Mazuk, S. "Adventures in Modeling Thermal Emission Spectra of Comets," (INVITED), *Proceedings of NASA conference, Thermal Emission Spectroscopy and Analysis of Dust, Disks and Regoliths*, Sitko, M. L., A. Sprague and D. K. Lynch (eds), 127–166, Astronomical Society of the Pacific, Conference Series 196, San Francisco (2000).

Mazuk, S. and D. K. Lynch, "Comparison of MODTRAN and FASCODE for Selection of a Cirrus Cloud Detection Band Near the 1.38 Micron Water Absorption Window," TR-2001(8570)-13, The Aerospace Corporation.

Mazuk, S., Lynch, D. K., Morgan, J. A., "On the Possibility of Detecting and Characterizing Thin Cirrus from Space in the 1–6 μm Region," TOR-2000(8570)-1, The Aerospace Corporation.

Takano, Y., Liou, K. N., Minnis, P., "The effects of small ice crystals on Cirrus Infrared Radiative Properties," *Journal of the American Meteorological Society*, **49** (16), pp. 1487–1493.

Shettle, E. P., Kneizys, F. X., Clough, S. A., Anderson, G. P., Abreu, L. W., and Chetwynd, J. H., 1986, "Cloud Models in LOWTRAN and FASCODE," Prc. CIDOS-1988 Workshop, D. Grantham and J. W. Snow (Eds.), 199–206.

van de Hulst, H.C., *Light Scattering by Small Particles*, Wiley, NY, 1957; Dover, NY, (1981).

Warren, S. G. "Optical constants of ice from the ultraviolet to the microwave," *Appl. Opt.*,**23**, 1026–1225, (1984).

LABORATORY OPERATIONS

The Aerospace Corporation functions as an "architect-engineer" for national security programs, specializing in advanced military space systems. The Corporation's Laboratory Operations supports the effective and timely development and operation of national security systems through scientific research and the application of advanced technology. Vital to the success of the Corporation is the technical staff's wide-ranging expertise and its ability to stay abreast of new technological developments and program support issues associated with rapidly evolving space systems. Contributing capabilities are provided by these individual organizations:

Electronics and Photonics Laboratory: Microelectronics, VLSI reliability, failure analysis, solid-state device physics, compound semiconductors, radiation effects, infrared and CCD detector devices, data storage and display technologies; lasers and electro-optics, solid state laser design, micro-optics, optical communications, and fiber optic sensors; atomic frequency standards, applied laser spectroscopy, laser chemistry, atmospheric propagation and beam control, LIDAR/LADAR remote sensing; solar cell and array testing and evaluation, battery electrochemistry, battery testing and evaluation.

Space Materials Laboratory: Evaluation and characterizations of new materials and processing techniques: metals, alloys, ceramics, polymers, thin films, and composites; development of advanced deposition processes; nondestructive evaluation, component failure analysis and reliability; structural mechanics, fracture mechanics, and stress corrosion; analysis and evaluation of materials at cryogenic and elevated temperatures; launch vehicle fluid mechanics, heat transfer and flight dynamics; aerothermodynamics; chemical and electric propulsion; environmental chemistry; combustion processes; space environment effects on materials, hardening and vulnerability assessment; contamination, thermal and structural control; lubrication and surface phenomena.

Space Science Applications Laboratory: Magnetospheric, auroral and cosmic ray physics, wave-particle interactions, magnetospheric plasma waves; atmospheric and ionospheric physics, density and composition of the upper atmosphere, remote sensing using atmospheric radiation; solar physics, infrared astronomy, infrared signature analysis; infrared surveillance, imaging, remote sensing, and hyperspectral imaging; effects of solar activity, magnetic storms and nuclear explosions on the Earth's atmosphere, ionosphere and magnetosphere; effects of electromagnetic and particulate radiations on space systems; space instrumentation, design fabrication and test; environmental chemistry, trace detection; atmospheric chemical reactions, atmospheric optics, light scattering, state-specific chemical reactions and radiative signatures of missile plumes.

Center for Microtechnology: Microelectromechanical systems (MEMS) for space applications; assessment of microtechnology space applications; laser micromachining; laser-surface physical and chemical interactions; micropropulsion; micro- and nanosatellite mission analysis; intelligent microinstruments for monitoring space and launch system environments.

Office of Spectral Applications: Multispectral and hyperspectral sensor development; data analysis and algorithm development; applications of multispectral and hyperspectral imagery to defense, civil space, commercial, and environmental missions.